Power-law Rheology in the Bulk and at the Interface: Quasi-Properties and Fractional Constitutive Equations.

Aditya Jaishankar and Gareth H. McKinley*

Department of Mechanical Engineering, Massachusetts Institute of Technology

77 Massachusetts Avenue, Cambridge - MA 02139, USA

*Corresponding Author: gareth@mit.edu

Consumer products like foods contain numerous polymeric and particulate additives that play critical roles in maintaining their stability, quality and function. The resulting materials exhibit complex bulk and interfacial rheological responses, and often display a distinctive power-law response under standard rheometric deformations. These power-laws are not conveniently described using conventional rheological models, without the introduction of a large number of relaxation modes. We present a constitutive framework utilizing fractional derivatives to model the power-law responses often observed experimentally. We first revisit the concept of quasi-properties and their connection to the fractional Maxwell model (FMM). Using Scott-Blair's original data, we demonstrate the ability of the FMM to capture the power-law response of 'highly anomalous' materials. We extend the FMM to describe the viscoelastic interfaces formed by bovine serum albumin and solutions of a common food stabilizer, Acacia gum. Fractional calculus allows us to model and compactly describe the measured frequency response of these interfaces in terms of their quasi-properties. Finally, we demonstrate the predictive ability of the FMM to quantitatively capture the behaviour of complex viscoelastic interfaces by combining the measured quasi-properties with the equation of motion for a complex fluid interface to describe the damped inertio-elastic oscillations that are observed experimentally.

Keywords: globular proteins; power-law; fractional Maxwell; Scott-Blair; creep ringing

1 Introduction

A multitude of consumer products, especially foods, owe their structure, stability and function to the presence of interfaces. Common examples include foams and emulsions such as milk, soups, salad dressings, mayonnaise, ice cream and butter (see McClements (2005) and the references therein). Although many of these foams and emulsions are thermodynamically unstable, the kinetics of phase separation can be controlled with the addition of various proteins, surfactants, gums and other stabilizing agents, which have very important implications for the shelf-life of foods (Murray (2002)). However, the presence of these additives often leads to complex rheological properties and give rise to distinctive power-laws in the creep response (i.e. the strain varies as $\gamma(t) \sim t^{\alpha}$) and also in the corresponding frequency response (i.e. the elastic modulus varies with frequency as $G'(\omega) \sim \omega^{\alpha}$). Such power-law responses are not well described by canonical rheological models such as the Maxwell or Kelvin-Voigt models (Tschoegl (1989)). The sensory perception of foods in terms of textural parameters plays an important role in the assessment of food quality, and is strongly related to the viscoelastic properties of the interfacial layers present (Fischer and Windhab (2011)). New rheological tools such as the double wall ring (DWR) interfacial rheometer (Vandebril et al. (2010); Jaishankar

et al. (2011)) enable us to experimentally quantify such responses with unprecedented accuracy over a wide range of frequency and time scales. We now seek a framework for modeling these power-law responses in a simple yet robust constitutive theory that can then be used to predict the material response in other, more complex, flows.

Constitutive modeling in rheology often involves constructing models that can be viewed conceptually as an arrangement of elastic Hookean springs and viscous Newtonian dashpots. Tschoegl (1989) compiles many such arrangements along with their response to various applied deformations. The canonical example is the linear viscoelastic Maxwell model, which consists of a spring and a dashpot in series. When a step strain deformation is imposed, the stress in the material responds exponentially, and this fundamental mode of response is commonly referred to as the *Maxwell-Debye Response* (Metzler and Klafter (2002)). Some model complex fluids (for example entangled worm-like micellar solutions in the fast-breaking chain limit) are well described by this simple model (Rehage and Hoffmann (1988)). However, there are many classes of materials in which stress relaxation following a step strain is not close to exponential, but is in fact best represented as a power-law in time, i.e. $G(t) \sim t^{-\beta}$. Examples of such materials include physically crosslinked polymers (Winter and Mours (1997)), microgel dispersions (Ketz et al. (1988)), foams (Khan et al. (1988)), colloidal hard sphere suspensions (Mason and Weitz (1995)), soft glassy materials (Sollich (1998)) and hydrogels (Larson (1999)). Non-exponential stress relaxation in the time domain also implies power-law behaviour in the viscoelastic storage modulus, $G'(\omega)$, and loss modulus, $G''(\omega)$, measured in the frequency domain using small amplitude oscillatory shear deformations. This broad spectral response is indicative of the wide range of distinct relaxation processes available to the microstructural elements that compose the material, and there is no single characteristic relaxation time (Metzler and Klafter (2002)). The irregular nature of relaxation events in complex fluids such as foods and consumer products is also often manifested in micro-rheological experiments as anomalous sub-diffusion or sticky diffusion, in which the mean square displacement of Brownian tracer particles is found to scale as $\langle x^2 \rangle \sim t^\alpha$, $0 < \alpha < 1$ (Metzler and Klafter (2000); Rich et al. (2011)).

To describe these so-called *power-law materials*, one may add progressively more mechanical elements in series or parallel to the initial Maxwell element or Voigt element (Tschoegl (1989)), and in the process provide additional modes of relaxation. We thus obtain a broad spectrum of discrete relaxation times that characterize the material response. Most real systems can thus be described in an *ad-hoc* way using a sum of exponentials Winter (1986). However for power-law materials to be modeled accurately, it is often found that a very large number of corresponding mechanical elements are required. For many complex fluids, this approach is frequently impractical from a modeling point of view. Moreover, the values of the fitted parameters in any model with a finite array of relaxation modes depend on the timescale of the experiment over which the fit is performed. Consequently the model parameters obtained lack physical meaning (Kollmannsberger and Fabry (2011)).

Scott-Blair (1947) pioneered a framework that enabled the power-law equation proposed by Nutting (1921) to be made more general through the use of fractional calculus. With analogy to the classical ideas of (i) the Hookean spring, in which the stress in the spring is proportional to the zero-th derivative of the strain and (ii) the Newtonian dashpot, in which the stress in the dashpot is proportional to the first derivative of the strain, he proposed a constitutive equation in terms of a *fractional derivative*

$$\sigma(t) = \mathbb{V} \frac{d^\alpha \gamma(t)}{dt^\alpha} \tag{1.1}$$

where $0 < \alpha < 1$, effectively creating an element that interpolates between the constitutive

responses of a spring and a dashpot. Here the material property $\mathbb{V}$ is a *quasi-property*, and d^α/dt^α is the fractional derivative operator (Miller and Ross (1993)), both of which are discussed in further detail below. Scott-Blair and co-workers used equation (1.1) as a constitutive equation in itself; Koeller (1984) later equated this canonical modal response to a mechanical element called the *spring-pot* (sometimes known as the Scott-Blair element (Mainardi and Gorenflo (2008))) and identified it as the fundamental building block from which more complex constitutive models could be constructed.

One of the consequences of Scott-Blair and coworkers' detailed study into these so-called fractional models is the emergence of the concept of material *quasi-properties*, denoted in equation (1.1) by the quantity $\mathbb{V}$ (with SI units of Pa s$^\alpha$). Quasi-properties differ from material to material in the dimensions of mass M, length L and time T, depending on the power α. It may thus be argued that they are not true material properties because they contain non-integer powers of the fundamental dimensions of space and time. However, such quasi-properties appear to compactly describe textural parameters such as the "firmness" of a material (Scott-Blair and Coppen (1942)). They are numerical measures of a dynamical process such as creep in a material rather than of an equilibrium state. In the present paper we show how we can compactly represent the wide range of microstructural relaxation processes in the material in terms of these so-called quasi-properties and the associated fractional derivatives with only a few parameters.

Bagley and Torvik (1983b) were able to demonstrate that, for long chain molecules with many submolecules per chain, the Rouse molecular theory (Rouse (1953)) is equivalent to a fractional constitutive equation, and compactly represented the polymer contribution to the total stress in terms of the fractional half-derivative of the strain. The Fractional Maxwell Model (FMM) and other fractional constitutive models have been considered in detail in the literature (Koeller (1984); Nonnenmacher (1991); Schiessel and Blumen (1993); Schiessel et al. (1995); Friedrich et al. (1999)).

We demonstrate in this paper that fractional stress-strain relationships are also applicable to viscoelastic interfaces, and result in simple constitutive models that may be used to quantitatively describe the power-law rheological behaviour exhibited by such interfaces. We first briefly outline the basic definitions of fractional calculus in a form most useful for applications in rheology. We then connect the framework to the studies of Scott-Blair and coworkers (Scott-Blair and Coppen (1942); Scott-Blair et al. (1947)) and show, using Scott-Blair et al.'s (1947) original data on 'highly anomalous butyl rubber', how the use of the fractional Maxwell model to extract the quasi-properties of this material is superior to the use of conventional spring-dashpot models that characterize creep and stress-relaxation. Next, we emphasize the utility of fractional constitutive models, and highlight the shortcomings of linear constitutive models for describing complex fluid interfaces using of interfacial rheology data obtained from highly viscoelastic bovine serum albumin and Acacia gum interfaces. Finally, we present a discriminating comparison of linear and fractional viscoelastic constitutive models using the phenomenon of creep ringing that arises from the coupling between surface elasticity and instrument inertia. We show that combining fractional constitutive models with the concept of material quasi-properties enables the quantitative description of complex time-dependent interfacial phenomena.

2   Mathematical preliminaries

(a)   Definitions

In this paper, we use the Caputo derivative for fractional differentiation, which is defined as Podlubny (1999); Surguladze (2002))

$$
{}_a^C\mathbf{D}_t^\alpha f(t) = \frac{1}{\Gamma(n-\alpha)} \int\limits_a^t (t-t')^{n-\alpha-1} f^{(n)}(t')dt' \tag{2.1}
$$

where $n-1 < \alpha \le n$, n is an integer and $f^{(n)}(t)$ indicates an integer order differentiation of the function $f(t)$ to order n. The Caputo derivative operator ${}_a^C\mathbf{D}_t^\alpha f(t)$ is itself a linear operator, so that ${}_a^C\mathbf{D}_t^\alpha[bf(t)+g(t)] = b\,{}_a^C\mathbf{D}_t^\alpha f(t) + {}_a^C\mathbf{D}_t^\alpha g(t)$ where b is any scalar and f and g are appropriate functions (Miller and Ross (1993)). In what follows, we choose the lower limit of integration $a = 0$, which us enables to reformulate the Caputo definition as a Laplace convolution (Schiessel et al. (1995)). In essence, we restrict our attention to the domain $t > 0$, because $f(t) = 0$ for $t \le 0$. Consequently, we henceforth use the more compact notation for the Caputo derivative:

$$
{}_0^C\mathbf{D}_t^\alpha f(t) \equiv \frac{d^\alpha}{dt^\alpha} f(t) \tag{2.2}
$$

The Laplace transform of the Caputo derivative is given by (Podlubny (1999))

$$
\mathcal{L}\left\{\frac{d^\alpha}{dt^\alpha} f(t); s\right\} = s^\alpha \tilde{f}(s) - \sum_{k=0}^{n-1} s^{\alpha-k-1} f^{(k)}(0), \ \ n-1 < \alpha \le n \tag{2.3}
$$

where $\tilde{f}(s) = \mathcal{L}\{f(t); s\}$. The Fourier transform of the Caputo derivative is given by (Schiessel et al. (1995))

$$
\mathcal{F}\left\{\frac{d^\alpha}{dt^\alpha} f(t); \omega\right\} = (i\omega)^\alpha \tilde{f}(\omega) \tag{2.4}
$$

where $\tilde{f}(\omega) = \mathcal{F}\{f(t); \omega\}$. Using these definitions, we can now formulate the FMM for a complex fluid, which is the simplest general rheological model involving spring-pots, and contains only four constitutive parameters.

(b)   The fractional Maxwell model - FMM

The spring-pot, whose constitutive equation is given in equation (1.1), bridges the gap between a purely viscous and a purely elastic material response by interpolating between a spring and a dashpot. For dimensional consistency, the constant $\mathbb{V}$ must have the units (Pa s$^\alpha$) where $0 \le \alpha \le 1$, and can be equated to Scott-Blair's concept of a quasi-property (Scott-Blair et al. (1947)). The formulation of fractional constitutive equations in terms of quasi-properties has fallen out of use in the recent rheological literature. It is often preferred to write the constitutive equation of a spring-pot (equation (1.1)) as $\sigma_{spring-pot} = G_0\lambda_0^\alpha \frac{d^\alpha \gamma}{dt^\alpha}$, where the modulus G_0 has units of [Pa] and λ_0 has units of [s] (see for example Friedrich and Braun (1992)). While this initially seems simply to be a matter of notational convenience, the latter formulation draws attention away from the fact that the fundamental material property that characterizes the behaviour of power-law–like materials is the unique quasi-property $\mathbb{V} = G_0\lambda_0^\alpha$, which characterizes the magnitude of the material response in terms of a single material parameter. In fact it can be shown that it is not possible from simple rheological tests to isolate the individual
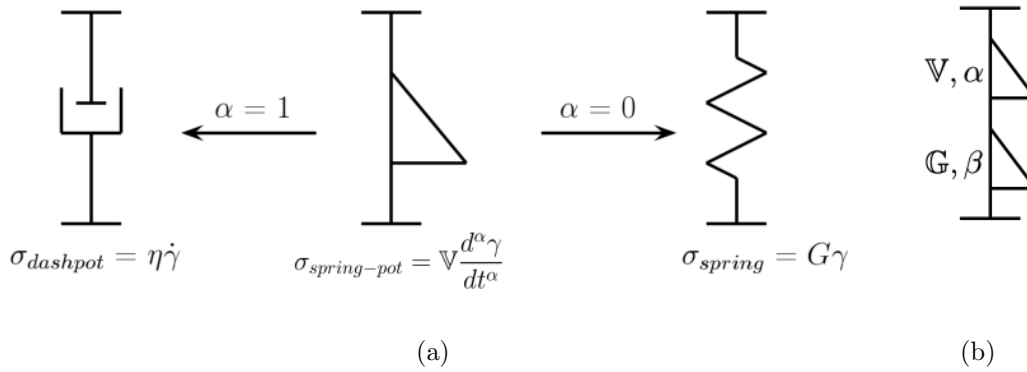
$$\sigma_{dashpot} = \eta\dot{\gamma}$$

$$\sigma_{spring-pot} = \mathbb{V}\frac{d^{\alpha}\gamma}{dt^{\alpha}}$$

$$\sigma_{spring} = G\gamma$$

$\mathbb{V}, \alpha$

$\mathbb{G}, \beta$

(a)   (b)

Figure 1: (a) The schematic representation of a spring-pot as an element that interpolates between a spring ($\alpha = 0$) and a dashpot ($\alpha = 1$). (b) The Fractional Maxwell Model (FMM).

components (G_0, λ_0, α), but only the product $G_0\lambda_0^{\alpha}$.

The two parameters $\mathbb{V}$ and α are the only parameters required to characterize a spring-pot. It is evident that the spring-pot—schematically shown in figure 1a—reduces to a spring when $\alpha = 0$ and a dashpot when $\alpha = 1$. The quasi-property $\mathbb{V}$ also reduces respectively to the limits of a modulus G (units: Pa) or a viscosity η (units: [Pa s]) in these limiting cases. The preferred term proposed by Scott-Blair et al. (1947) for a constitutive law exhibiting spring-pot like behaviour was "the principle of intermediacy". We present a vectorial graphical representation of the spring-pot in the electronic supplementary material to aid in understanding this intermediate nature of the spring-pot.

We may now use these spring-pot elements to construct more complex constitutive models. This approach has been discussed in some detail in the literature, notably by Bagley and Torvik (1983a), Torvik and Bagley (1984), Koeller (1984), Nonnenmacher (1991), Friedrich (1991a), Schiessel and Blumen (1993) and Heymans and Bauwens (1994); we therefore summarize the primary result without derivation. The FMM consists of two spring-pots in series characterized by the parameters $(\mathbb{V}, \alpha)$ and $(\mathbb{G}, \beta)$ respectively (figure 1b). The constitutive equation for the FMM can be obtained from assuming equality of the stress ($\sigma = \sigma_1 = \sigma_2$) in the spring-pots, and additivity of the strains ($\gamma = \gamma_1 + \gamma_2$) to give

$$\sigma(t) + \frac{\mathbb{V}}{\mathbb{G}}\frac{d^{\alpha-\beta}\sigma(t)}{dt^{\alpha-\beta}} = \mathbb{V}\frac{d^{\alpha}\gamma(t)}{dt^{\alpha}} \tag{2.5}$$

where we take $\alpha > \beta$ without loss of generality (Schiessel et al. (1995)). The ratio $(\mathbb{V}/\mathbb{G})^{1/(\alpha-\beta)}$ with units of [s] represents the fractional generalization of a characteristic relaxation time for the model.

Friedrich (1991b) has shown that this model results in a nonnegative internal work and a nonnegative rate of energy dissipation, and is hence consistent with the laws of thermodynamics. Lion (1997) has argued more generally that a constitutive model containing fractional elements is thermodynamically admissible only if the resulting constitutive equation represents some physically realizable combination of springs, dashpots and spring-pots. In other words, models that do not have mechanical analogues are thermodynamically inadmissible.

In a stress relaxation experiment, a step strain of the form $\gamma = \gamma_0 H(t)$ is imposed (where $H(t)$ is the Heaviside step function) and the stress is measured as a function of time. The solution of equation (2.5) following the imposition of such a step strain can be solved analytically

and the relaxation modulus is expressed as (Schiessel et al. (1995))

$$G(t) \equiv \frac{\sigma(t)}{\gamma_0} = \mathbb{G}t^{-\beta}E_{\alpha-\beta,1-\beta}\left(-\frac{\mathbb{G}}{\mathbb{V}}t^{\alpha-\beta}\right) \tag{2.6}$$

where $E_{a,b}(z)$ is the two parameter Mittag-Leffler function defined as (Podlubny (1999))

$$E_{a,b}(z) = \sum_{k=0}^{\infty}\frac{z^k}{\Gamma(ak+b)}, \qquad\qquad (a>0, b>0) \tag{2.7}$$

Note that in equation (2.6) we have written the expression for $G(t)$ in terms of the quasi-properties $\mathbb{G}$ and $\mathbb{V}$ of the two spring-pot elements, and the power-law exponents α, β.

We may also analytically solve for the compliance $J(t)$ in a creep experiment in where a step stress of the form $\sigma(t) = \sigma_0 H(t)$ is imposed, where σ_0. Substituting this equation into the fractional Maxwell constitutive equation (equation (2.5)), we can now solve for the evolution of the strain in the Laplace domain. We note that the necessary initial conditions are determined from the fact that the sample is initially at rest, and we have $\dot{\gamma}(0) = 0$. Moreover, the state of zero strain may be fixed arbitrarily, and we set the material strain to be $\gamma(0) = 0$ at $t = 0$. Hence, upon inverting the Laplace transformed strain $\tilde{\gamma}(s)$ we arrive at

$$J(t) \equiv \frac{\gamma(t)}{\sigma_0} = \left(\frac{1}{\mathbb{V}}\frac{t^\alpha}{\Gamma(1+\alpha)} + \frac{1}{\mathbb{G}}\frac{t^\beta}{\Gamma(1+\beta)}\right) \tag{2.8}$$

where $\Gamma(z)$ is the Gamma function. It is evident that setting $\alpha = 1$ and $\beta = 0$ retrieves the creep response of the linear viscoelastic Maxwell model given by $J(t) = \left(\frac{t}{\eta} + \frac{1}{G}\right)$.

In this paper, we are interested in the properties of complex interfaces. Because interfacial stresses correspond to a line force, they have units of [Pa m] or [N/m]. This additional length dimension also influences the units of the corresponding interfacial quasi-properties $\mathbb{V}_s, \mathbb{G}_s$ that characterize complex interfaces, and they now have units of Pa m s$^\alpha$ and Pa m s$^\beta$ respectively, which remain quasi-properties in time. To construct a constitutive equation for complex fluid interfaces, we write the interfacial counterpart of equation (2.5) as

$$\sigma_s(t) + \frac{\mathbb{V}_s}{\mathbb{G}_s}\frac{d^{\alpha-\beta}\sigma_s(t)}{dt^{\alpha-\beta}} = \mathbb{V}_s\frac{d^\alpha\gamma(t)}{dt^\alpha} \tag{2.9}$$

in which $\sigma_s(t)$ is the interfacial stress (Any symbol in this paper with the subscript 's' is to be interpreted as an interfacial quantity unless otherwise specified). This model is confronted with experimental data in §4 of the present paper.

3   Techniques and materials

To demonstrate the ability of the fractional models discussed above to describe viscoelastic interfaces, we performed interfacial rheological experiments on bovine serum albumin (BSA) and Acacia gum solutions. Interfacial rheological experiments were performed with a TA Instruments ARG2 stress-controlled rheometer using the double wall ring (DWR) fixture. The construction and operation of the DWR has been described in detail by Vandebril et al. (2010). The test fixture consists of a Platinum-Iridium ring that is placed at the air-liquid or liquid-liquid interface of interest. The ring has a square cross-section angled at 45° to pin the location of the interface and minimize the effects of meniscus curvature. Steady or oscillatory shear

deformations may be applied to the fluid interface using the DWR and the resulting torque is measured.

In any interfacial shear rheological experiment, torque contributions from the flow induced in the subphase are present in addition to the interfacial torque contribution. For accurate measurements, it is important to identify these subphase contributions and ensure that they do not dominate over the interfacial torque measurements. The selective sensitivity of a specific test geometry to interfacial effects, in comparison to the induced subphase flow, is characterized by the Boussinesq number Bo_s (Edwards et al. (1991)). For $Bo_s \gg 1$, interfacial effects dominate, and the length scale $l_s = A_B/P_s$ is thus crucial in determining the relative sensitivity of a particular fixture to interfacial viscous effects as compared to subphase effects from the bulk. In all our experiments, we ensured that this requirement is satisfied. The relatively small value of the length scale l_s for the DWR fixture as compared to other available rheometer fixtures leads to a higher value of the Boussinesq number. Additional details regarding the importance of the Boussinesq number in interfacial measurements are discussed elsewhere (Edwards et al. (1991); Sharma et al. (2011); Vandebril et al. (2010)).

Bovine serum albumin, extracted by agarose gel electrophoresis, was obtained from Sigma-Aldrich Corp (St. Louis, MO USA) in the form of a lypophilized powder. 0.01 M phosphate buffered saline (PBS) solution (NaCl 0.138 M; KCl 0.0027 M; pH 7.4, at 25 °C.) was prepared by dissolving dry PBS powder obtained from Sigma-Aldrich Corp. A precisely weighed quantity of BSA was dissolved in the PBS and the solution was brought up to the required volume in a volumetric flask to finally obtain solutions with a BSA concentration of 50 mg ml^{-1}. The uncertainty in composition from solution preparation was determined to be only 0.002%. The prepared solutions were stored under refrigeration at 4 °C and were allowed to slowly warm up to room temperature before being used for experiments. All BSA solutions used in this study had a concentration of 50 mg ml^{-1} unless otherwise specified.

Acacia gum in powdered form was also obtained from Sigma-Aldrich Corp (SKU:G9752). Using the same weighing technique described above, a known quantity of Acacia gum was dissolved in deionized water by slow stirring for approximately 6 hours to make solutions at a concentration of 3 wt.%. The solutions were then double-filtered using Whatman filter paper grade #595 (pore-size: $4-7~\mu$m) to remove any residual insoluble material. Prior to rheological testing, all solutions were stored at 4°C for 24 hours to ensure biopolymer hydration (Sanchez et al. (2002)).

4   Results

(a)   *Stress relaxation and creep without inertia*

We first consider the stress relaxation in a complex material after the imposition of a step strain. The broad spectrum of relaxation times exhibited by power-law materials often present challenges in modeling such experiments (Ng et al. (2011)). It has already been noted that the inclusion of additional relaxation modes, which is equivalent to including additional Maxwell or Voigt units in parallel, gives improved fits to experimental data. The resulting expression for linear viscoelastic stress relaxation is a Prony series (Larson (1999); Baumgartel and Winter (1992))

$$G(t) \equiv \frac{\sigma(t)}{\gamma_0} = \sum_{k=1}^{N_m} \frac{\eta_k}{\lambda_k} e^{-\frac{t}{\lambda_k}} \tag{4.1}$$

where η_k and λ_k are fitting constants. The number of modes N_m required to fit experimental data varies depending on the time scale over which the relaxation modulus is measured and the

degree to which the experimental data deviates from the exponential Maxwell-Debye response. Although describing data in this manner is a well-posed exercise, it is often cumbersome because of the large number of fitting parameters required. Tschoegl (1989) remarks presciently "If the number of Maxwell of Voigt units is increased to the minimum number required for a series-parallel model to represent such a [power-law] distribution at all adequately, the simplicity of the standard models is lost and, in addition, arbitrary decisions must be made in assigning suitable values to the model elements."

Another empirical approach often used to describe experimental observations of power-law–like relaxation is a stretched exponential response, known as the Kohlrausch-Williams-Watts expression (KWW) (Larson (1999)), given by $\sigma(t) = G\gamma_0 e^{-(t/\tau)^\beta}$ where the characteristic relaxation time τ, the exponent β and the modulus scale G are the fitting constants. The KWW expression works well in practice for describing the step strain excitation; However it is in general not possible using standard procedures to find the underlying form of the constitutive model that could subsequently be used to predict the response of the material to another mode of excitation (Tschoegl (1989)). Scott-Blair et al. (1947) attempted to model measurements of anomalous stress relaxation in a range of materials using a higher-order Nutting equation of the form

$$\gamma = \sigma^\beta (At^{k'} + Bt^{k'-1} + Ct^{k'-2} \dots) \tag{4.2}$$

with $A \gg B, C, \dots$. However, we show in the electronic supplementary information that this equation is not thermodynamically admissible.

To demonstrate the ability of properly-formulated fractional constitutive models and the resulting quasi-properties to compactly describe the complex time-dependent properties of real viscoelastic materials, we revisit Scott-Blair et al.'s original stress relaxation data and fit the measurements with the FMM discussed in §2(b). In figure 2 we re-plot representative data reported for the original stress relaxation and creep experiments performed by Scott-Blair et al. (1947). We to plot the relaxation modulus $G(t)$ and the corresponding creep compliance $J(t)$ for compactness, instead of the original stress and strain values respectively. It can be seen that the data collapse onto a rheological master-curve as expected for experiments performed in the limit of linear deformations. We now fit equation (2.6) to the measured $G(t)$ values shown in figure 2a. We set one of the elements in the FMM to be a spring, (i.e. $\beta = 0$); this accounts for the instantaneous elastic response in the stress at the start of the experiment. The FMM fit (solid line) describes the material response extremely well over a wide range of timescales (10 s $\leq t \leq$ 400 s) in terms of just three material parameters $\alpha = 0.60 \pm 0.04$, $\mathbb{V} = 2.7 \pm 0.7 \times 10^7$ Pa s$^{0.60}$ and $\mathbb{G} = 2.3 \pm 0.2 \times 10^6$ Pa, (with $\beta = 0$). The error bars in the figure and the error estimates of the individual parameters $\alpha, \mathbb{V}$ and $\mathbb{G}$ correspond to 95% confidence intervals for the nonlinear least square parameter fits. A satisfactory fit using a sum of relaxation modes (equation (4.1)) is obtained only if three relaxation modes are used, leading to the use of six fitting parameters, instead of the three required in the fractional Maxwell case.

If the values of the quasi-properties found above truly characterize the material, then we should be able to *predict* the constitutive response of the material to other deformations using the same rheological equation of state. To demonstrate this, we next consider the creep data for the same 'highly anomalous' rubber presented by Scott-Blair et al. (1947) which has been plotted as the creep compliance $J(t)$ in figure 2b. We can use equation (2.8) to predict the creep response of the 'highly anomalous' rubber based on the power-law exponent and quasi-properties found from fits to the relaxation modulus. Substituting these values into equation (2.8) leads to the solid curve shown in figure 2b. It can be seen that the prediction of
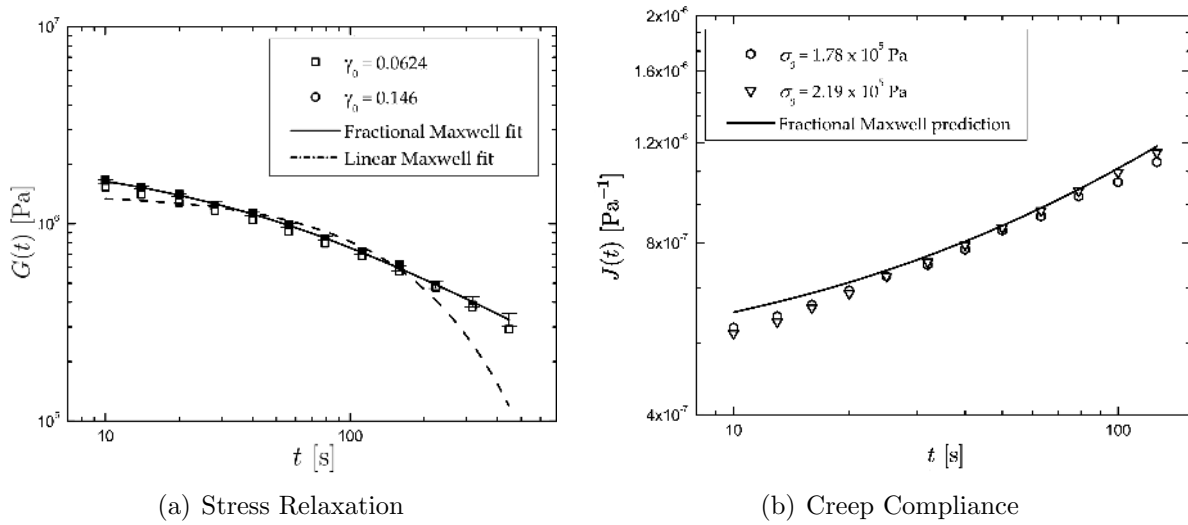
(a) Stress Relaxation

(b) Creep Compliance

Figure 2: Rheological data for 'highly anomalous' butyl rubber taken from Scott-Blair et al. (1947). (a) Representative data of stress relaxation experiments performed at two different strain amplitudes. The solid line depicts the FMM fit (equation (2.6)), with one of the elements set to be a spring ($\beta = 0$). For comparison, the fit obtained from a linear Maxwell model is shown as a dashed line. (b) Creep data at two different stresses for the same 'highly anomalous' butyl rubber. The solid line represents the prediction of the FMM (equation (2.8)) based on the quasi-properties determined from the stress relaxation fit.

the model again agrees very well with measured data, indicating that the FMM quantitatively describes the power-law–like behaviour observed by Scott-Blair in these 'anomalous' materials.

From this analysis of some previously-published data, the superiority of fractional models in compactly describing the broad power-law like response of real materials is apparent. Similar power-law creep responses are commonly observed in both microrheological experiments (Maloney et al. (2010); Rich et al. (2011)) and macroscopic experiments (Cameron et al. (2011); Erni et al. (2007)). Scott-Blair's concept of quasi-properties is intimately connected to the framework of fractional calculus models and provides a physical material interpretation of the predictive power of these apparently abstract constitutive models.

(b)   Interfacial dynamics

Interfacial rheology or '2D rheology' studies the dynamics and structure of interfacial viscoelastic thin films or skins formed by solutions containing surface active molecules (Edwards et al. (1991)). Understanding the mechanics of viscoelastic interfaces is critical to a number of applications including the use of food additives and stabilizers (Murray (2002)), medicine, physiology and pharmaceuticals (Zasadzinski et al. (2001); Leiske et al. (2010)). Although static surface tension measurements are sufficient to characterize the interfacial properties of surfactant-free solutions with clean interfaces, accurate descriptions of solutions or dispersions containing surface active molecules with dynamically evolving interfaces necessitate correct accounting of the mass and momentum transport processes occurring at the interface (Erni (2011)). In this paper, we will only concern ourselves with the interfacial response of surface-active solutions to shearing deformations, although dilatational interfacial phenomena can also be important in other modes of deformation (Cascão Pereira et al. (2003)).

Two common examples of surface active materials are Acacia gum solutions and BSA solutions, which form the focus of the present study. The surface characteristics of BSA solutions at the air-water interface have been studied extensively using multiple techniques and it is well established that these solutions form rigid viscoelastic interfaces (Biswas and Haydon (1963);
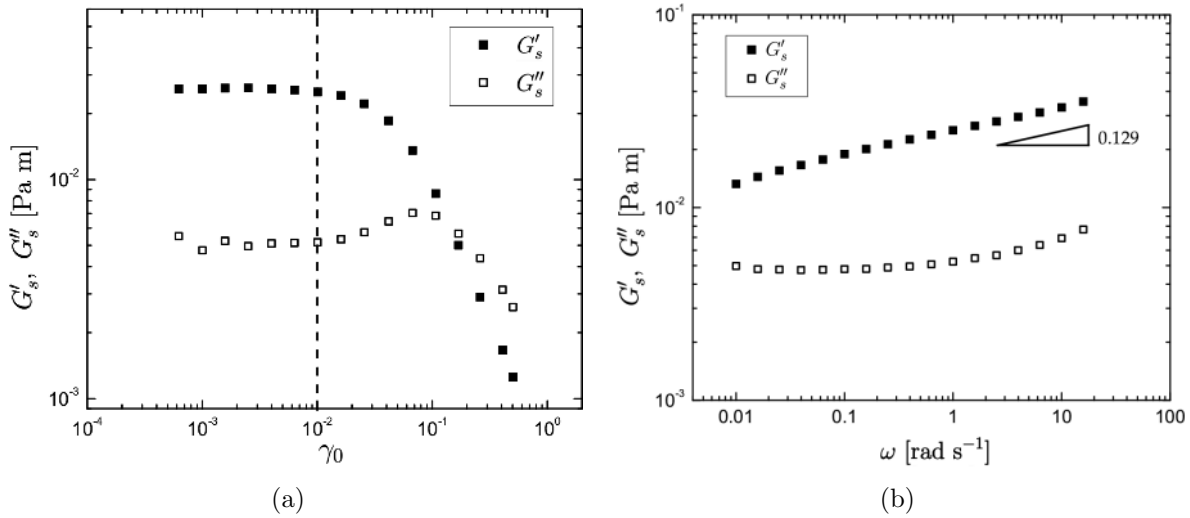
Figure 3: Interfacial small amplitude oscillatory shear data of 3 wt.% Acacia gum solutions carried out using the DWR. (a) Strain amplitude sweep performed at $\omega = 1$ rad s^{-1}. (b) Frequency sweep performed at a strain amplitude $\gamma_0 = 1\%$, which lies in the linear regime. The viscoelastic interface shows weak power-law behaviour with $G_s''(\omega)$ remaining nearly flat over the tested frequency range.

Graham and Phillips (1980); Cascão Pereira et al. (2003); Sharma et al. (2011)). On the other hand, although some interfacial studies have been performed on Acacia gum solutions (Dickinson et al. (1988); Erni et al. (2007); Elmanan et al. (2008)), there is comparatively less literature available for these solutions. Furthermore, there is significant variability present between Acacia gums extracted from different sources.

For each sample, we first performed interfacial time sweep experiments at a fixed frequency of $\omega = 1$ rad s^{-1} and a fixed strain amplitude of $\gamma_0 = 1$ % to monitor the time evolution of interfacial viscoelasticity at the interface. We find that the interfacial viscoelastic storage and loss moduli, $G_s'(\omega)$ and $G_s''(\omega)$ respectively, reach equilibrium about 2.5 hours after sample loading, indicating that the interfacial structure has reached steady-state. It is observed that $G_s'(\omega) > G_s''(\omega)$ indicating that the interfacial microstructures formed is predominantly elastic. The solid-like nature of the microstructures formed at the interface can also be observed in the strain sweep performed at an angular frequency of $\omega = 1$ rad s^{-1} shown in figure 3a. In the linear regime, we measure $G_s' \approx 0.025$ Pa m $> G_s'' \approx 5 \times 10^{-3}$ Pa m. The interfacial structure yields at a strain amplitude of about $\gamma_0 \approx 3\%$. In figure 3b we show the values of the interfacial moduli as a function of excitation frequency for the 3 wt.% Acacia gum solution. Throughout the frequency range tested, $G_s'(\omega) > G_s''(\omega)$ signifying that viscoelastic solid-like behaviour persists even at lower frequencies. Testing at frequencies lower than $\omega = 10^{-2}$ rad s^{-1} was avoided to prevent evaporation effects from interfering with the measurements. Erni et al. (2007) have reported that the values of G_s' and G_s'' measured in a frequency sweep are unchanged upon changing the concentration of Acacia gum in the subphase from 10 wt.% to 20 wt.%, which has been attributed to the saturation of the interface by Acacia gum molecules.

The viscoelastic data obtained from the frequency sweep exhibits a weak power-law behaviour, which is typical of many physical and chemical gels (Winter and Mours (1997)) as well as soft glassy materials (Sollich (1998)). Numerous recent reports of bulk rheology in soft solids have shown examples of such power-law behaviour in small amplitude oscillatory shear deformations (for example Holten-Andersen et al. (2011); Cameron et al. (2011); Kollmannsberger and Fabry (2011)). We have already demonstrated the utility of fractional models in describing

	$G_s'(\text{ Pa m})$		$G_s''(\text{ Pa m})$	
$\lim_{\omega \to 0}$	$\mathbb{V}_s\omega^\alpha \cos\left(\frac{\pi}{2}\alpha\right)$	, if $\alpha \neq 1$	$\mathbb{V}_s\omega^\alpha \sin\left(\frac{\pi}{2}\alpha\right)$	, if $\alpha \neq 0$
	$\frac{\mathbb{V}_s^2}{\mathbb{G}_s}\omega^{2-\beta} \cos\left(\frac{\pi}{2}\beta\right)$	, if $\alpha = 1$	$0 \ (\forall\omega)$	, if $\alpha = 0$
$\lim_{\omega \to \infty}$	$\mathbb{G}_s\omega^\beta \cos\left(\frac{\pi}{2}\beta\right)$	, if $\beta \neq 1$	$\mathbb{G}_s\omega^\beta \sin\left(\frac{\pi}{2}\beta\right)$	, if $\beta \neq 0$
	$0 \ (\forall\omega)$	, if $\beta = 1$	$\frac{\mathbb{G}_s^2}{\mathbb{V}_s}\omega^{-\alpha} \sin\left(\frac{\pi}{2}\alpha\right)$	, if $\beta = 0$

Table 1: Asymptotic behaviour of $G_s'(\omega)$ and $G_s''(\omega)$ in the FMM. Because $0 < \beta < \alpha < 1$, G_s' and G_s'' reduce identically to 0 for the cases $\beta = 1$ and $\alpha = 0$ respectively, and the result holds for all frequencies.

bulk creep and stress relaxation experiments in §4*(a)*. We next examine the ability of the FMM to describe the power-law responses observed in interfacial oscillatory deformations.

(c)   The FMM in small amplitude oscillatory shear (SAOS) deformations

The complex fluid examples discussed above, including the Acacia gum and bovine serum albumin interfaces tested in this study exhibit broad power-law responses when subjected to small amplitude oscillatory shear experiments. Winter and Mours (1997) have presented a model for critical gels in which the storage and loss moduli in the bulk are described by the power laws $G'(\omega) = S\Gamma(1-n)\cos(n\pi/2)\omega^n$ and $G''(\omega) = S\Gamma(1-n)\sin(n\pi/2)\omega^n$ respectively, where S is the gel strength parameter (units of Pa s^n). It may be shown by inverse Fourier transforming the complex modulus $G^*(\omega) = G'(\omega) + iG''(\omega)$ and finding the resulting constitutive equation that this is equivalent to a constitutive model consisting of a single spring-pot and the gel strength parameter is closely related to the quasi-property of the spring-pot $\mathbb{V} = S\Gamma(1-n)$.

One may achieve a more versatile constitutive model for describing foods and other gels and soft glasses that show power-law–like rheology by considering the FMM depicted schematically in figure 1b. For a viscoelastic interface the corresponding interfacial constitutive equation is equation (2.9). Following the procedure outlined by Friedrich (1991a), and Schiessel et al. (1995), we evaluate the complex modulus of the interface by Fourier transforming equation (2.9) using equation (2.4) to obtain

$$G_s^*(\omega) = \frac{\mathbb{V}_s(i\omega)^\alpha \cdot \mathbb{G}_s(i\omega)^\beta}{\mathbb{G}_s(i\omega)^\alpha + \mathbb{V}_s(i\omega)^\beta} \tag{4.3}$$

By evaluating the real and imaginary parts of the right-hand side of equation (4.3), we find that the storage and loss moduli are given, respectively, by

$$G_s'(\omega) = \frac{(\mathbb{G}_s\omega^\beta)^2 \cdot \mathbb{V}_s\omega^\alpha \cos\left(\frac{\pi}{2}\alpha\right) + (\mathbb{V}_s\omega^\alpha)^2 \cdot \mathbb{G}_s\omega^\beta \cos\left(\frac{\pi}{2}\beta\right)}{(\mathbb{V}_s\omega^\alpha)^2 + (\mathbb{G}_s\omega^\beta)^2 + 2\mathbb{V}_s\omega^\alpha \cdot \mathbb{G}_s\omega^\beta \cos\left(\frac{\pi}{2}(\alpha-\beta)\right)} \tag{4.4}$$

$$G_s''(\omega) = \frac{(\mathbb{G}_s\omega^\beta)^2 \cdot \mathbb{V}_s\omega^\alpha \sin\left(\frac{\pi}{2}\alpha\right) + (\mathbb{V}_s\omega^\alpha)^2 \cdot \mathbb{G}_s\omega^\beta \sin\left(\frac{\pi}{2}\beta\right)}{(\mathbb{V}_s\omega^\alpha)^2 + (\mathbb{G}_s\omega^\beta)^2 + 2\mathbb{V}_s\omega^\alpha \cdot \mathbb{G}_s\omega^\beta \cos\left(\frac{\pi}{2}(\alpha-\beta)\right)} \tag{4.5}$$

The asymptotic behaviours of equations (4.4) and (4.5) in the limit of low and high frequencies are given in table 1. Several different limits can be distinguished in the special cases corresponding to $\beta = 0, 1$ and $\alpha = 0, 1$ respectively. These limits reduce correctly to those of the linear Maxwell model when $\alpha = 1$ and $\beta = 0$. When multiple Maxwell modes are used to generate a satisfactory description of the behaviour of power-law materials, we often require a very large number of discrete relaxation times (Tschoegl (1989)), something that can be readily circumvented with the use of a fractional model such as equation (2.9). The fractional calculus

description captures the dynamics of the broad spectrum of relaxation times very succinctly, by collapsing them into a single spring-pot (Schiessel and Blumen (1993)).

One limitation of the critical gel model is that the elastic and viscous moduli remain parallel to each other over all frequencies, and the loss tangent $\tan \delta = \Gamma(1 - n)$ is independent of frequency. In contrast, many experiments show broad power-law signatures over some frequency range but ultimately a cross-over at low enough frequencies to a limiting viscous-like material response. The existence of a characteristic relaxation time in the FMM (see equation (2.9)) enables such a material response to be described. The crossover frequency ω_c at which $G'_s = G''_s$ for the FMM is found by equating equations (4.4) and (4.5) and we then find

$$\omega_c = \left(\frac{\mathbb{G}_s}{\mathbb{V}_s} \left[\frac{\sin \frac{\pi}{2}\alpha - \cos \frac{\pi}{2}\alpha}{\cos \frac{\pi}{2}\beta - \sin \frac{\pi}{2}\beta} \right] \right)^{\frac{1}{\alpha - \beta}} \tag{4.6}$$

Equation (4.6) makes it evident that the characteristic relaxation timescale in this model is $\tau \simeq \omega_c^{-1} \sim (\mathbb{V}_s/\mathbb{G}_s)^{\frac{1}{\alpha - \beta}}$, provided the argument in square brackets is positive. However there is no crossover predicted by the model if $0 < \beta < \alpha < 0.5$ or if $0.5 < \beta < \alpha < 1$ (the total model response is then predominantly elastic or viscous, respectively, at all frequencies). For such materials no clear characteristic timescale exists.

In figure 4 we show SAOS measurements of the interfacial viscoelasticity for 3 wt. % Acacia gum solutions and 50 mg/ml BSA solutions. The black solid lines in figures 4a and 4c show the fit of the FMM for the elastic interfacial modulus $G'_s(\omega)$ (equation (4.4)) for the 3 wt.% Acacia gum solutions and 50 mg/ml BSA solutions respectively. The dashed lines show the predicted values of the interfacial loss modulus $G''_s(\omega)$ (equation (4.5)). From these fits, the power-law exponents that characterize the Acacia gum solution are determined to be $\alpha = 0.8 \pm 0.2, \beta = 0.124 \pm 0.003$, and the corresponding quasi-properties are $\mathbb{V}_s = 3 \pm 2$ Pa m s$^{0.8}$, $\mathbb{G}_s = 0.027 \pm 0.003$ Pa m s$^{0.124}$. The material parameters of the 50 mg/ml BSA solution are $\alpha = 0.80 \pm 0.07, \beta = 0.11 \pm 0.02, \mathbb{V}_s = 0.048 \pm 0.008$ Pa m s$^{0.80}$, $\mathbb{G}_s = 0.017 \pm 0.001$ Pa m s$^{0.11}$. When the loss modulus is plotted against the storage modulus in a Cole-Cole representation, we do not observe the simple semicircular response expected from a linear Maxwell material but instead power-law materials produce Cole-Cole plots with more complicated elliptical shapes (Friedrich and Braun (1992)). It can be seen from the figures that the FMM captures the frequency dependence of the interfacial material functions accurately. On the other hand, the single-mode linear Maxwell model (indicated by broken lines in figures 4b and 4d) is unable to capture the power-law behaviour of these viscoelastic interfaces.

It is possible to estimate the crossover point and hence the relaxation time of the viscoelastic interface from the FMM fit. Calculating the value of ω_c using equation (4.6), we find that for the Acacia gum solution $\omega_c = 7.0 \times 10^{-4}$ rad s^{-1} corresponding to a characteristic time constant of $t_c \approx 1430$ s. As we have noted previously, it is challenging to measure linear viscoelastic properties at such low frequencies and at room temperature due to the long times it takes for test completion, which can result in solvent evaporation. In the case of the BSA solutions the interfacial relaxation time is shorter and the crossover point can be measured directly using the DWR fixture giving $\omega_c = 0.16$ rad s^{-1} ($t_c \approx 6.4$ s). This crossover to a viscously dominated response is also captured accurately by the FMM. Acacia gum clearly produces a predominantly elastic interface with a very long relaxation time.

The values of the interfacial quasi-properties of the Acacia gum and BSA solutions we have found here fully characterize the linear viscoelastic interfacial properties of the two solutions, and these parameters may now be used to predict the response of these rheologically complex
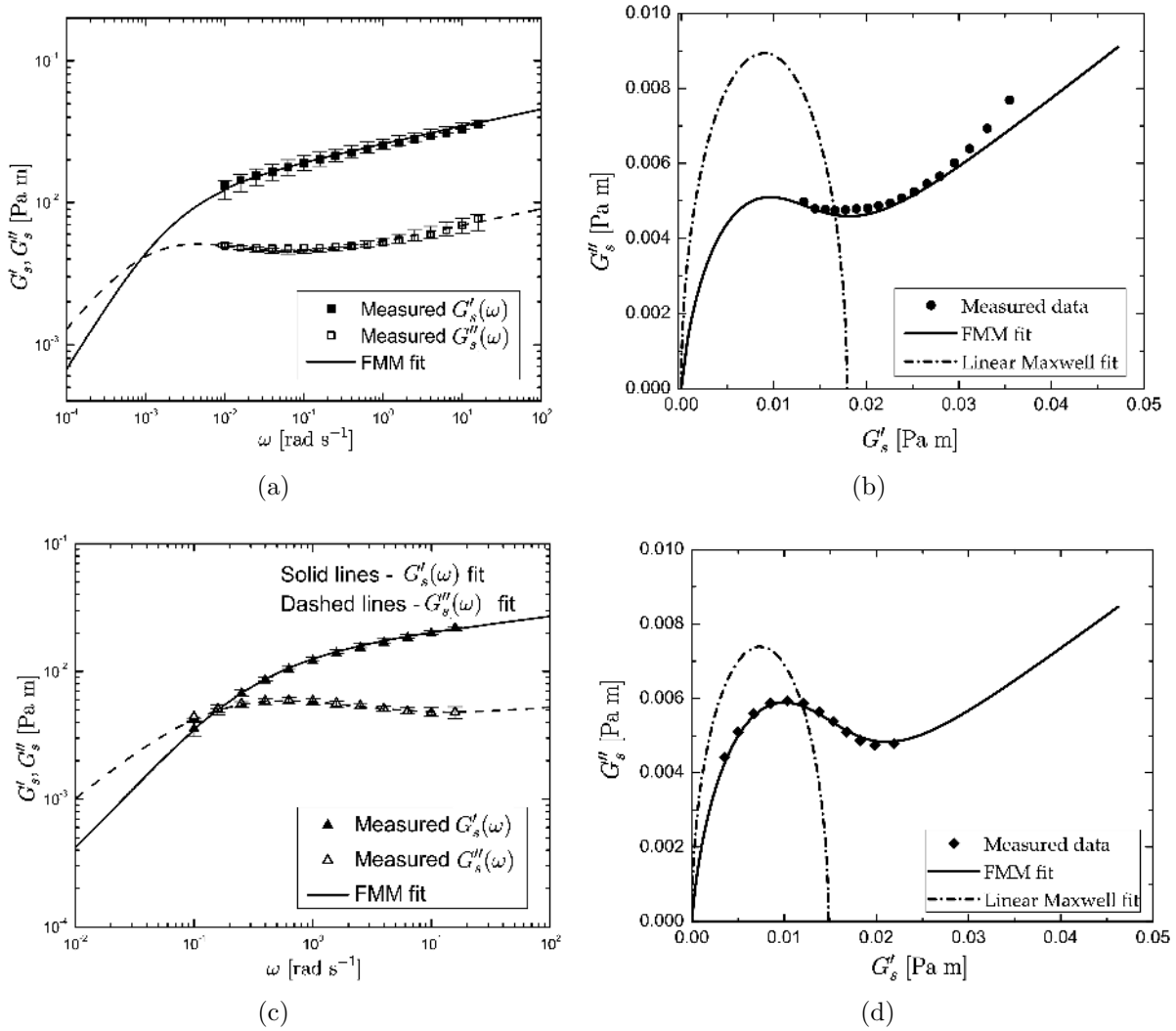
Figure 4: The FMM fitted (lines) to interfacial storage $G'_s(\omega)$ and loss $G''_s(\omega)$ moduli data (symbols) obtained from (a),(b) 3 wt.% Acacia gum solutions and (c),(d) 50 mg/ml BSA solutions. $G'_s(\omega)$. The FMM fits are given by equation (4.4) and equation (4.5) respectively. Cole-Cole plot of (b) the same Acacia gum solution and (d) BSA solution showing the fractional Maxwell fit as a solid line with a linear Maxwell fit shown for comparison by the dashed line. The values of the exponents and quasi-properties extracted from the fit are given in the main text.

materials to other modes of excitation. In the next subsection we discuss the transient response of the materials in creep experiments when inertial effects in the flow cannot be neglected.

(d) Creep ringing and power-law responses

In stress controlled bulk rheometry, the effects of inertia can be coupled with material elasticity which leads to damped periodic oscillations in a step-stress experiment at early times (Baravian and Quemada (1998); Ewoldt and McKinley (2007)). We have shown in a previous study that this inertio-elastic phenomenon can be observed not just in the bulk but at interfaces as well (Jaishankar et al. (2011)). These periodic oscillations decay exponentially with time due to viscous dissipation, and this phenomenon is often termed creep-ringing. Although the presence of these oscillations is generally regarded as an intrusion, these transients can, in fact, be exploited to extract useful information about the linear viscoelasticity of soft materials (Baravian and Quemada (1998); Ewoldt and McKinley (2007)). In previous work using BSA
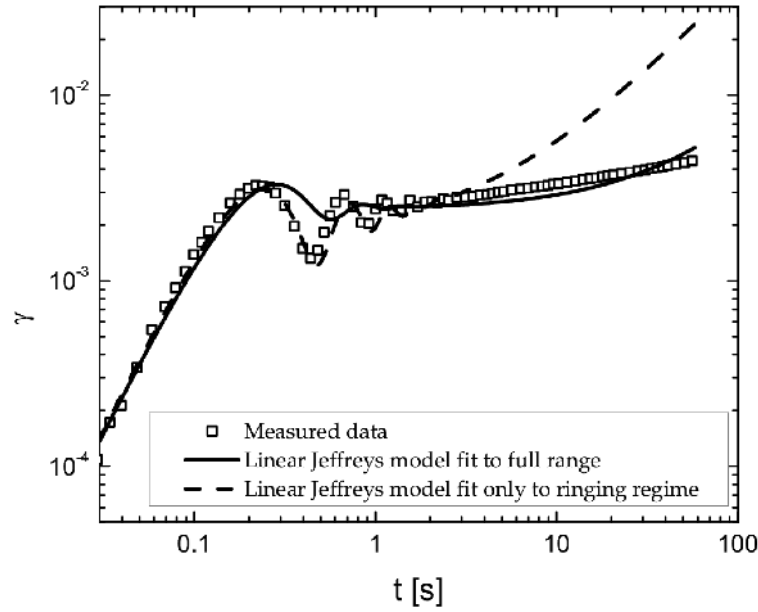
Figure 5: Interfacial creep data obtained with a 50 mg/ml BSA solution. A viscously damped inertio-elastic ringing is present at early times and a power-law behaviour is exhibited at long times. The solid line shows the linear Maxwell fit to the entire time range of the experiment, and the dashed line shows the linear Maxwell fit only to the ringing regime. Neither fit performs adequately at capturing both the ringing phenomenon as well as the long-time power-law behaviour.

solutions exhibiting interfacial viscoelasticity (Jaishankar et al. (2011)), we have shown that this technique of extracting interfacial properties even presents certain advantages over the conventional technique of conducting frequency sweep measurements to high frequencies. In this earlier study we also noted that solutions of BSA exhibit a power-law creep response at long times, which could not be adequately captured with the linear Maxwell-Jeffreys model that was considered analytically. In figure 5 we show a creep experiment performed on 50 mg/ml BSA solutions with significant inertial effects as well as the best fit prediction of the Maxwell-Jeffreys model (Tschoegl (1989)) with an added inertial mass. The damped oscillatory ringing arising from the interaction of the fluid viscoelasticity with instrument inertial effects can be observed at short times, and power-law creep behaviour is seen in the experimental data at long times. The solid black line shows the best fit to a linear Jeffreys model performed on the full temporal span of the creep data ($0.02 \leq t \leq 60$ s). Although the long time ($t \geq 1$ s) fit is acceptable, the fit to the inertio-elastic ringing regime is poor. Moreover, the best fit increasingly deviates at longer times. On the other hand, a fit performed only to the creep-ringing regime ($0 \leq t \leq 1$ s), shown by the black dashed line, predicts the material response poorly at long times. In the current work, we extend the creep ringing analysis to fractional viscoelastic constitutive models for the interface; we aim to predict the power-law creep behaviour over the entire time range of the experiment using the material power exponents and quasi-properties determined previously in frequency sweep experiments (figure 4).

In figure 6 we show measurements of the interfacial creep compliance $J_s(t)$ (with units of [Pa^{-1} m^{-1}]) of 3 wt. % Acacia gum solutions for different values of the imposed interfacial stress σ_s^0. We observe that the interfacial compliance $J_s(t) \equiv \gamma(t)/\sigma_s^0$ measured at different stresses collapse onto a single curve indicating the measurements are in the linear viscoelastic regime. The inset plot shows the creep compliance response at long times on logarithmic axes, which exhibits a power-law scaling in time with $J_s(t) \sim t^{0.13}$, instead of the slope of unity or zero expected from, respectively, a purely viscous or purely elastic material response.
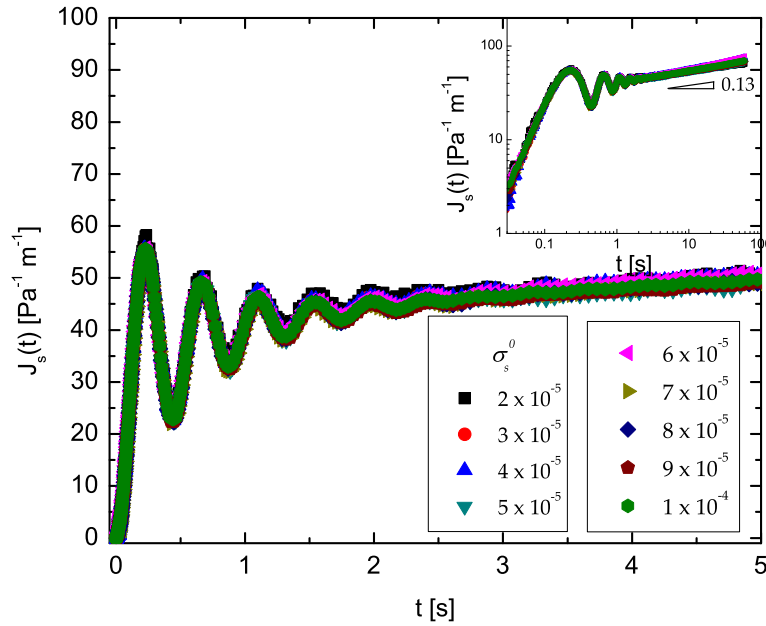
Figure 6: Creep compliance for 3 wt.% Acacia gum solutions performed at various values of imposed interfacial stress σ_s^0. All experiments collapse onto a single curve as expected for a linear viscoelastic response. The interfacial viscoelasticity is coupled with instrument inertia giving rise to creep ringing at early times. The inset plot shows that at long times the creep compliance at exhibits power-law behaviour with $J_s(t) \sim t^{0.13}$. (Online version in colour).

To overcome the poor predictions achieved from single mode linear viscoelastic models, and without resorting to the *ad-hoc* introduction of a large number of superposed relaxation modes, we instead use the FMM (equation (2.9)) coupled with the inertia of the test fixture to describe both the ringing observed in the creep experiment at short times, as well as the power-law behaviour seen at long times. We begin with the equation of the motion of the spindle of the stress-controlled rheometer, (Baravian and Quemada (1998); Ewoldt and McKinley (2007))

$$\frac{I}{b_s}\frac{d^2\gamma}{dt^2} = H(t)\sigma_s^0 - \sigma_s(t) \tag{4.7}$$

where I is the total moment of inertia of the spindle of the rheometer and the attached test geometry (i.e. the DWR fixture), $\sigma_s(t)$ is the retarding interfacial stress applied by the sample on the spindle and $\gamma(t)$ is the resulting strain. The factor $b_s = F_\gamma/F_\sigma$ (units of m^2) is a geometric factor determined by the specific instrument and geometry used. The quantities $F_\gamma = \dot{\gamma}/\Omega$ (dimensionless) and $F_\sigma = \sigma_s/T$ (units: m^{-2}) convert the measured quantities of torque T and angular velocity Ω into the rheologically-relevant quantities of interfacial stress σ_s and strain rate $\dot{\gamma}$ respectively. Equation (4.7) can now be coupled with equation (2.5) to yield the fractional differential equation

$$\mathbb{V}_s\frac{d^\alpha\gamma}{dt^\alpha} + A\frac{\mathbb{V}_s}{\mathbb{G}_s}\frac{d^{2+\alpha-\beta}\gamma}{dt^{2+\alpha-\beta}} = H(t)\sigma_s^0 + \frac{\mathbb{V}_s}{\mathbb{G}_s}\frac{d^{\alpha-\beta}}{dt^{\alpha-\beta}}H(t)\sigma_s^0 \tag{4.8}$$

where we introduce $A = I/b_s$ for compactness. In the above equation we have used the composition rule for fractional derivatives, which states that $\frac{d^q}{dt^q}\frac{d^p f}{dt^p} = \frac{d^{p+q}f}{dt^{p+q}}$ provided $f^{(k)}(0) = 0$ where $k = 0, 1, \dots, m-1$; $m < p < m+1$ (Podlubny (1999)). The fractional differential equation (4.8) is of order $2 + \alpha - \beta$, and Heymans and Podlubny (2006) have shown that a

fractional differential equation of arbitrary real order k requires k^* initial conditions, where k^* is the lowest integer greater than k. Because we have $0 \leq \beta \leq \alpha \leq 1$, we find that we need three initial conditions. The spindle is initially at rest and hence $\gamma(0) = \dot{\gamma}(0) = 0$. However the step in stress causes an instantaneous acceleration and the third initial condition is $\sigma_s(0) = 0$ which is equivalent to $\ddot{\gamma}(0) = \sigma_s^0/A$ from equation (4.7).

Before we solve equation (4.3) for $\gamma(t)$, we first seek to determine its asymptotic behaviour in the limits of early times and long times. Evaluating the Laplace transform of equation (4.8) using equation (2.3) and employing the three initial conditions given above, we find that

$$\tilde{\gamma}(s) = \frac{\sigma_s^0}{s} \left(\frac{1 + \frac{\mathbb{V}_s}{\mathbb{G}_s} s^{\alpha - \beta}}{\mathbb{V}_s s^\alpha + As^2 + A\frac{\mathbb{V}_s}{\mathbb{G}_s} s^{2+(\alpha-\beta)}} \right) \tag{4.9}$$

It may be shown (see the electronic supplementary material) that at short times equation (4.9) yields

$$\gamma(t)|_{t\to 0} \approx \frac{1}{2} \frac{\sigma_s^0}{A} t^2 + \cdots \tag{4.10}$$

This quadratic response is independent of the fractional orders of the spring-pots α and β as expected, because the short time response in the equation of motion (4.7) is dictated solely by the inertial response of the fixture; at very early times the interface has not had time to build-up any stress and hence $\sigma_s(t) \approx 0$. The solution of equation (4.7) under the condition $\sigma_s(t) = 0$ yields the quadratic expression in equation (4.10). Similarly, at long times we obtain (see the electronic supplementary material for details)

$$\gamma(t)|_{t\to\infty} \approx \sigma_s^0 \left(\frac{t^\alpha}{\mathbb{V}_s \Gamma(\alpha + 1)} + \frac{t^\beta}{\mathbb{G}_s \Gamma(\beta + 1)} \right) + \cdots \tag{4.11}$$

which is, to the leading order, the same as the inertia-free creep response derived in equation (2.8). This means that the effects of inertia become unimportant at long times, as observed in the experimental measurements shown in figure 6.

The value of $A = I/b_s$ can be calibrated once the rheometer fixture is selected and in our case was found to be $A = 1.72 \times 10^{-4}$ kg. Figure 7 shows the asymptotic short time response (line) given by equation (4.10) plotted against the measured interfacial creep compliance of a 3 wt. % Acacia gum solution (filled symbols). It can be seen that the short time asymptotic response agrees very well with the measured data. The inset plot also shows the value of the long time asymptote derived in equation (4.11). From the fractional Maxwell Cole-Cole fits shown in figure 4, the fit values that characterize the Acacia gum solutions are found to be $\alpha = 0.8 \pm 0.2, \beta = 0.124 \pm 0.003, \mathbb{V}_s = 3 \pm 2$ Pa s$^{0.8}$, $\mathbb{G}_s = 0.027 \pm 0.003$ Pa s$^{0.124}$. Because $\frac{t^\beta}{\mathbb{G}_s} \approx 6\frac{t^\alpha}{\mathbb{V}_s}$ at $t = 60$ s, we find that the first term in equation (4.11) is smaller than the second. Therefore, to a first approximation, at long times $\gamma(t) \approx \frac{\sigma_s^0}{\mathbb{G}_s} \frac{t^\beta}{\Gamma(1+\beta)}$. Calculating the value of the coefficient $\frac{1}{\mathbb{G}_s \Gamma(1+\beta)}$, we find it equals 39.3 Pa^{-1} m^{-1} s$^{-0.124}$. When we fit a power-law of the form $\gamma(t) = at^b$ directly to the measured data, where a and b are fitting constants, we find that the measured data at long times is described by $J_s(t) \approx 40.4t^{0.130}$ Pa^{-1} m^{-1}, which is in excellent agreement with the analytically derived asymptotic predictions for long times. This asymptotic power-law creep behaviour, shown as the solid line in the inset plot in figure 7, cannot be conveniently captured using conventional spring-dashpot models.

We now proceed to predict the interfacial creep response of the Acacia gum solutions based
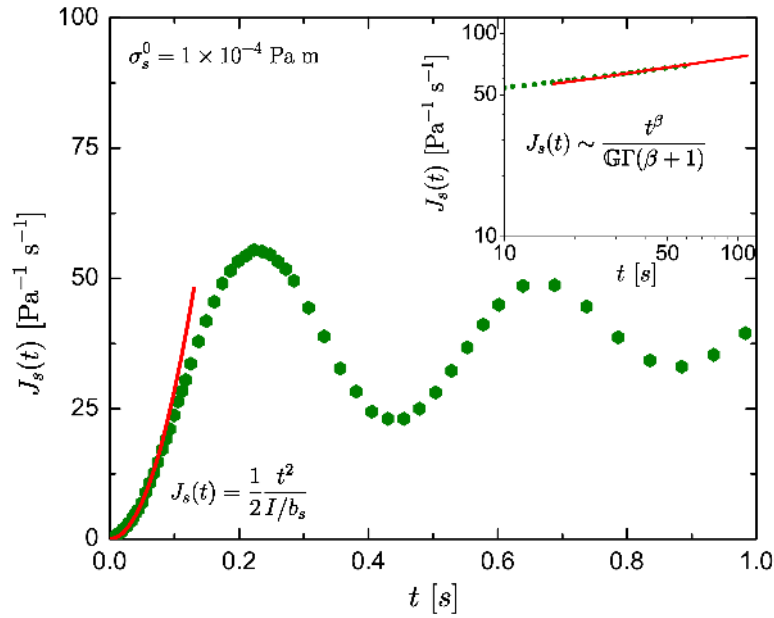
Figure 7: Experimentally measured values of the interfacial compliance response (symbols), and the short and long time asymptote in the FMM coupled with instrument inertia. At early times, we retrieve the expected quadratic response of $J_s(t) \sim \frac{1}{2}\frac{t^2}{I/b_s}$ which is in accordance with the equation of motion at very early times. At long times, the effect of inertia only appears as a higher order correction (equation (4.11)). (Online version in colour).

on the FMM fit parameters and quasi-properties found in §4(c). To this end, we solve equation (4.8) for the strain $\gamma(t)$ with the values of $\mathbb{V}_s, \mathbb{G}_s, \alpha$ and β determined from the fits of the FMM to the small amplitude oscillatory shear data. Equation (4.8) is amenable to an analytical solution and can be found by calculating the inverse Laplace transform of equation (4.9), in terms of the Mittag-Leffler function defined in equation (2.7). However the resulting expression is cumbersome to evaluate because it contains a double infinite sum. Instead, we circumvent this difficulty by solving equation (4.8) numerically using the procedure outlined by Podlubny et al. (2009) and a modified version of a MATLAB code freely available from the same group. We refer the reader to the paper by Podlubny et al. (2009) for details of the numerical scheme used.

The resulting numerical solution of equation (4.8) obtained using the quasi-properties found from SAOS is plotted in figure 8 as a solid line overlaid onto the experimentally measured compliance data. It is observed that the prediction of $J_s(t)$ based on the previously fitted quasi-property values is in very good agreement with the measured temporal response over the entire range of the creep experiment, indicating that the quasi-properties of the FMM characterize the rheological response of the material over a wide range of timescales. This fractional constitutive model can predict the response to other excitations once the quasi-properties have been found from SAOS fits. This would not be possible using empirical laws such as the KWW expression, or the critical gel equation, although these laws are able to capture power-law behaviour. It is noteworthy that the FMM contains only two additional parameters (α, β) beyond a simple Kelvin or Maxwell response and yet enables excellent predictions accounting for the damped inertio-elastic effects at short times as well as the long time power-law response.
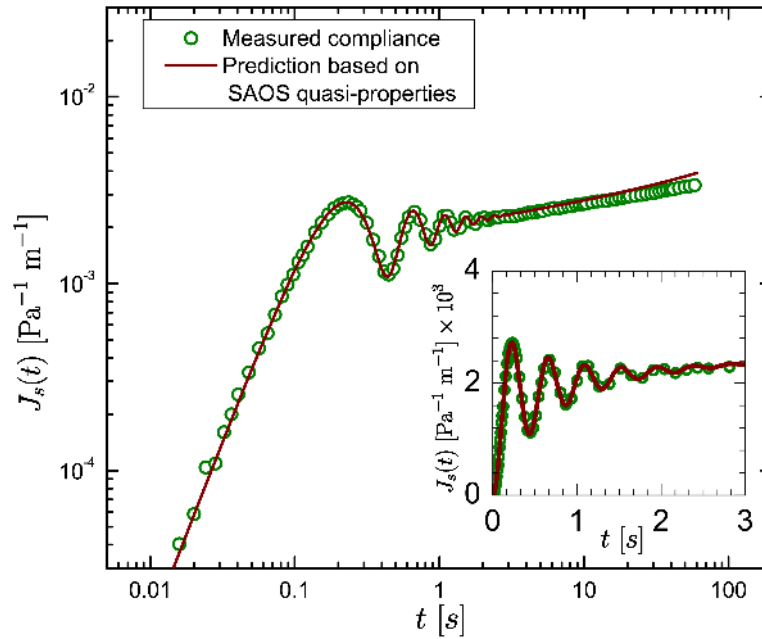
Figure 8: The predicted interfacial creep compliance from solving equation (4.8) numerically using the exponents and quasi-properties found from the SAOS experiments that characterize the Acacia gum solutions. The prediction made by the model is in excellent agreement with the measured data, and it captures both the creep ringing at early times as well as the power-law behaviour observed at long times. (Online version in colour).

5   Conclusions

We have revisited the concept of quasi-properties for describing the rheology of complex microstructured materials and interfaces, and demonstrated how their inclusion in fractional constitutive models containing spring-pot mechanical elements leads to the natural and quantitative description–using only a few constitutive parameters–of power-law behaviour frequently observed experimentally. Not only is this fractional constitutive approach more compact than the traditional approach of using a multi-mode Prony series, it is also more physical; in the latter approach, the number of fitted parameters as well as their magnitudes depend on the timescale of the experiment used for model fitting.

In the spring-pot constitutive equation, the elastic modulus, $G'(\omega)$, and the loss modulus, $G''(\omega)$, increase as a function of frequency while maintaining a constant ratio between them. This is reminiscent of the behaviour observed in critical gels and soft glassy materials (Sollich (1998)). In fact it can be shown that the soft glassy rheology (SGR) model under certain conditions yields exactly the same constitutive relationship as a single spring-pot defined in the Caputo sense, and the 'effective noise temperature' x in the SGR model is intimately related to the fractional exponent α (or β). Both these aspects are discussed in the electronic supplementary information.

Not only can fractional models accurately model the complex relaxation behaviour exhibited by bulk materials (as demonstrated here using Scott-Blair's (1947) original data on 'highly anomalous' butyl rubber), they can also be extended to describe complex viscoelastic interfaces as well. Using small amplitude oscillatory shear experiments, we measured the power-law linear viscoelastic behaviour exhibited by interfaces formed from adsorbed films of bovine serum albumin and Acacia gum. By fitting the data to the FMM, we could extract the quasi-properties $\mathbb{V}_s$, $\mathbb{G}_s$ and exponents α, β that characterize these rheologically-complex interfaces. We then considered the transient flow generated by an interfacial creep experiment in which inertial

contributions are significant. We were able to predict *a priori* the inertio-elastic creep ringing observed at short times as well as the long-time power-law response using the values of the quasi-properties determined previously. There is excellent agreement between the model predictions and the experimental data across a wide range of timescales. These measurements demonstrate that once the quasi-properties of a material have been determined from one particular excitation they characterize this rheologically-complex interface and help determine the material response to other modes of deformation.

Finally we note that all of the models presented here describe the linear viscoelastic limit and cannot describe non-linear viscoelastic behaviour (for example the onset of shear thinning or strain softening) exhibited by many complex fluids and interfaces at large strains. Extending the capability of fractional constitutive models into the non-linear regime remains an open research problem for future investigation.

References

R. L. Bagley and P. J. Torvik. Fractional calculus - A different approach to the analysis of viscoelastically damped structures. *AIAA Journal*, 21(5):741–748, May 1983a. doi: 10.2514/3.8142.

R. L. Bagley and P. J. Torvik. A theoretical basis for the application of fractional calculus to viscoelasticity. *Journal of Rheology*, 27(3):201, 1983b.

C. Baravian and D. Quemada. Using instrumental inertia in controlled stress rheometry. *Rheologica Acta*, 37 (3):223–233, June 1998. doi: 10.1007/s003970050110.

M. Baumgartel and H. H. Winter. Interrelation between discrete and continuous relaxation spectra. In P. Moldenaers and R. Keunings, editors, *Proc. XIth Int. Congr. on Rheology*, pages 893–895, 1992.

B. Biswas and D. A. Haydon. The rheology of some interfacial adsorbed films of macromolecules. I. Elastic and creep phenomena. *Proceedings of the Royal Society A: Mathematical, Physical and Engineering Sciences*, 271 (1346):296–316, Jan. 1963. doi: 10.1098/rspa.1963.0019.

A. R. Cameron, J. E. Frith, and J. J. Cooper-White. The influence of substrate creep on mesenchymal stem cell behaviour and phenotype. *Biomaterials*, 32:5979–5993, May 2011. doi: 10.1016/j.biomaterials.2011.04.003.

L. G. Cascão Pereira, O. Théodoly, H. W. Blanch, and C. J. Radke. Dilatational Rheology of BSA Conformers at the Air/Water Interface. *Langmuir*, 19(6):2349–2356, Mar. 2003. doi: 10.1021/la020720e.

E. Dickinson, B. S. Murray, G. Stainsby, and D. M. W. Anderson. Surface activity and emulsifying behaviour of some Acacia gums. *Food Hydrocolloids*, 2:477–490, 1988.

D. A. Edwards, H. Brenner, and D. T. Wasan. *Interfacial Transport Processes and Rheology*. Butterworth-Heinemann, Boston, 1991.

M. Elmanan, S. Al-Assaf, G. O. Phillips, and P. A. Williams. Studies on Acacia exudate gums: Part VI. Interfacial rheology of Acacia senegal and Acacia seyal. *Food Hydrocolloids*, 22:682–689, 2008. doi: http://dx.doi.org/10.1016/j.foodhyd.2007.02.008.

P. Erni. Deformation modes of complex fluid interfaces. *Soft Matter*, 7(17):7586, 2011. doi: 10.1039/c1sm05263b.

P. Erni, E. J. Windhab, R. Gunde, M. Graber, B. Pfister, A. Parker, and P. Fischer. Interfacial rheology of surface-active biopolymers: Acacia senegal gum versus hydrophobically modified starch. *Biomacromolecules*, 8(11):3458–66, Nov. 2007. doi: 10.1021/bm700578z.

R. H. Ewoldt and G. H. McKinley. Creep ringing in rheometry or how to deal with oft-discarded data in step stress tests! *Rheology Bulletin*, 76(1):4–6, 2007.

P. Fischer and E. J. Windhab. Rheology of food materials. *Current Opinion in Colloid & Interface Science*, 16 (1):36–40, Feb. 2011. doi: 10.1016/j.cocis.2010.07.003.

C. Friedrich. Relaxation and retardation functions of the Maxwell model with fractional derivatives. *Rheologica Acta*, 30(2):151–158, 1991a.

C. Friedrich. Relaxation functions of rheological constitutive equations with fractional derivatives: thermodynamical constraints. In *Rheological Modelling: Thermodynamical and Statistical Approaches*, pages 321–330. Springer-Verlag, 1991b.

C. Friedrich and H. Braun. Generalized Cole-Cole behavior and its rheological relevance. *Rheologica Acta*, 31: 309–322, 1992.

C. Friedrich, H. Schiessel, and A. Blumen. Constitutive Behavior Modeling and Fractional Derivatives. In D. A. Siginer, D. De Kee, and R. P. Chhabra, editors, *Advances in the flow and rheology of non-newtonian fluids*, pages 429–266. 1999.

D. E. Graham and M. C. Phillips. Proteins at Liquid Interfaces V. Shear properties. *Journal of Colloid and Interface Science*, 76(1):240–250, Dec. 1980.

N. Heymans and J. C. Bauwens. Fractal rheological models and fractional differential equations for viscoelastic behavior. *Rheologica Acta*, 33(3):210–219, 1994. doi: 10.1007/BF00437306.

N. Heymans and I. Podlubny. Physical interpretation of initial conditions for fractional differential equations with Riemann-Liouville fractional derivatives. *Rheologica Acta*, 45(5):765–771, Nov. 2006. doi: 10.1007/ s00397-005-0043-5.

N. Holten-Andersen, M. J. Harrington, H. Birkedal, B. P. Lee, P. B. Messersmith, K. Y. C. Lee, and J. H. Waite. pH-induced metal-ligand cross-links inspired by mussel yield self-healing polymer networks with near-covalent elastic moduli. *Proceedings of the National Academy of Sciences of the United States of America*, 108(7):2651–5, Feb. 2011. doi: 10.1073/pnas.1015862108.

A. Jaishankar, V. Sharma, and G. H. McKinley. Interfacial viscoelasticity, yielding and creep ringing of globular protein-surfactant mixtures. *Soft Matter*, 7(17):7623–7634, 2011. doi: 10.1039/c1sm05399j.

R. J. Ketz, R. K. Prud'homme, and W. W. Graessley. Rheology of concentrated microgel solutions. *Rheologica Acta*, 27(5):531–539, Sept. 1988. doi: 10.1007/BF01329353.

S. A. Khan, C. A. Schnepper, and R. C. Armstrong. Foam rheology: III. Measurement of shear flow properties. *Journal of Rheology*, 32(1):69–92, 1988.

R. C. Koeller. Applications of Fractional Calculus to the Theory of Viscoelasticity. *Journal of Applied Mechanics*, 51(2):299–307, 1984. doi: 10.1115/1.3167616.

P. Kollmannsberger and B. Fabry. Linear and Nonlinear Rheology of Living Cells. *Annual Review of Materials Research*, 41(1):75–97, Aug. 2011. doi: 10.1146/annurev-matsci-062910-100351.

R. G. Larson. *The Structure and Rheology of Complex Fluids*. Oxford University Press, New York, 1999.

D. L. Leiske, S. R. Raju, H. A. Ketelson, T. J. Millar, and G. G. Fuller. The interfacial viscoelastic properties and structures of human and animal Meibomian lipids. *Experimental Eye Research*, 90(5):598–604, May 2010. doi: 10.1016/j.exer.2010.02.004.

A. Lion. On the thermodynamics of fractional damping elements. *Continuum Mechanics and Thermodynamics*, 9(2):83–96, 1997.

F. Mainardi and R. Gorenflo. Time-fractional derivatives in relaxation processes: a tutorial survey. *Arxiv preprint arXiv:0801.4914*, 10(3):269–308, 2008.

J. M. Maloney, D. Nikova, F. Lautenschläger, E. Clarke, R. Langer, J. Guck, and K. J. Van Vliet. Mesenchymal stem cell mechanics from the attached to the suspended state. *Biophysical journal*, 99(8):2479–87, Oct. 2010. doi: 10.1016/j.bpj.2010.08.052.

T. G. Mason and D. A. Weitz. Linear viscoelasticity of colloidal hard sphere suspensions near the glass transition. *Physical Review Letters*, 75(14):2770–2773, Oct. 1995.

D. J. McClements. *Food Emulsions: Principles, Practices, and Techniques*. CRC Press, 2005.

R. Metzler and J. Klafter. The random walk's guide to anomalous diffusion: A fractional dynamics approach. *Physics Reports*, 339:1–77, 2000.

R. Metzler and J. Klafter. From stretched exponential to inverse power-law: fractional dynamics, Cole-Cole relaxation processes, and beyond. *Journal of Non-Crystalline Solids*, 305(1):81–87, 2002.

K. S. Miller and B. Ross. *An Introduction to the Fractional Calculus and Fractional Differential Equations*. John Wiley & Sons, Inc., 1993.

B. S. Murray. Interfacial rheology of food emulsifiers and proteins. *Current Opinion in Colloid & Interface Science*, 7(5-6):426–431, Nov. 2002. doi: 10.1016/S1359-0294(02)00077-8.

T. S. K. Ng, G. H. McKinley, and R. H. Ewoldt. Large amplitude oscillatory shear flow of gluten dough: A model power-law gel. *Journal of Rheology*, 55(3):627, 2011. doi: 10.1122/1.3570340.

T. Nonnenmacher. Fractional relaxation equations for viscoelasticity and related phenomena. *Rheological Modelling: Thermodynamical and Statistical Approaches*, (7):309–320, 1991.

P. Nutting. A new general law of deformation. *Journal of the Franklin Institute*, 191(5):679–685, 1921.

I. Podlubny. *Fractional Differential Equations*. Academic Press, San Diego, 1999.

I. Podlubny, T. Skovranek, and B. M. Vinagre Jara. Matrix approach to discretization of fractional derivatives and to solution of fractional differential equations and their systems. In *2009 IEEE Conference on Emerging Technologies & Factory Automation*, pages 1–6. Ieee, Sept. 2009. ISBN 978-1-4244-2727-7. doi: 10.1109/

ETFA.2009.5347166.

H. Rehage and H. Hoffmann. Rheological properties of viscoelastic surfactant systems. *The Journal of Physical Chemistry*, 92(16):4712–4719, 1988.

J. P. Rich, G. H. McKinley, and P. S. Doyle. Size dependence of microprobe dynamics during gelation of a discotic colloidal clay. *Journal of Rheology*, 55(2):273, 2011. doi: 10.1122/1.3532979.

P. E. Rouse. A theory of the linear viscoelastic properties of dilute solutions of coiling polymers. *The Journal of Chemical Physics*, 21(7):1272, 1953. doi: 10.1063/1.1699180.

C. Sanchez, D. Renard, P. Robert, C. Schmitt, and J. Lefebvre. Structure and rheological properties of acacia gum dispersions. *Food Hydrocolloids*, 16(3):257–267, 2002. doi: DOI:10.1016/S0268-005X(01)00096-0.

H. Schiessel and A. Blumen. Hierarchical analogues to fractional relaxation equations. *Journal of Physics A: Mathematical and General*, 26:5057–5069, 1993.

H. Schiessel, R. Metzler, A. Blumen, and T. Nonnenmacher. Generalized viscoelastic models: their fractional equations with solutions. *Journal of Physics A: Mathematical and General*, 28:6567–6584, 1995.

G. W. Scott-Blair. The role of psychophysics in rheology. *J. Colloid Science*, 2:21–32, 1947.

G. W. Scott-Blair and F. Coppen. The subjective conception of the firmness of soft materials. *The American Journal of Psychology*, 55(2):215–229, 1942.

G. W. Scott-Blair, B. C. Veinoglou, and J. E. Caffyn. Limitations of the Newtonian time scale in relation to non-equilibrium rheological states and a theory of quasi-properties. *Proceedings of the Royal Society A: Mathematical, Physical and Engineering Sciences*, 189(1016):69–87, Mar. 1947. doi: 10.1098/rspa.1947.0029.

V. Sharma, A. Jaishankar, Y.-C. Wang, and G. H. McKinley. Rheology of globular proteins: apparent yield stress, high shear rate viscosity and interfacial viscoelasticity of bovine serum albumin solutions. *Soft Matter*, 7(11):5150–5160, 2011. doi: 10.1039/c0sm01312a.

P. Sollich. Rheological constitutive equation for a model of soft glassy materials. *Physical Review E*, 58(1): 738–759, 1998.

T. Surguladze. On certain applications of fractional calculus to viscoelasticity. *Journal of Mathematical Sciences*, 112(5):4517–4557, 2002.

P. J. Torvik and R. L. Bagley. On the appearance of the fractional derivative in the behavior of real materials. *Journal of Applied Mechanics*, 51(2):294, 1984. doi: 10.1115/1.3167615.

N. W. Tschoegl. *The Phenomenological Theory of Linear Viscoelastic Behavior.* Springer-Verlag, Berlin, 1989.

S. Vandebril, A. Franck, G. G. Fuller, P. Moldenaers, and J. Vermant. A double wall-ring geometry for interfacial shear rheometry. *Rheologica Acta*, 49(2):131–144, Dec. 2010. doi: 10.1007/s00397-009-0407-3.

H. H. Winter. Analysis of linear viscoelasticity of a crosslinking polymer at the gel point. *Journal of Rheology*, 1986.

H. H. Winter and M. Mours. Rheology of polymers near liquid-solid transitions. In *Advances in Polymer Science, Vol. 134*, pages 165–234. Springer-Verlag, 1997.

J. A. Zasadzinski, J. Ding, H. E. Warriner, F. Bringezu, and A. J. Waring. The physics and physiology of lung surfactants. *Current Opinion in Colloid & Interface Science*, 6(5-6):506–513, Nov. 2001. doi: 10.1016/S1359-0294(01)00124-8.